SPATIAL COUPLING OF MULTIBODY SYSTEM WITH VISCOUS FLOW DYNAMICS IN PARTITIONED ALGORITHMS

Dubravko Matijašević, **Zdravko Terze**

Department of Aeronautical Engineering
Faculty of Mechanical Engineering and Naval Architecture, University of Zagreb
Ivana Lučića 5, 10000 Zagreb, Croatia

Abstract

Mathematical model and numerical procedure of multibody system in fluid flow is used in weakly coupled approach to simulate forward dynamics of wing with aileron model. Multibody system (MBS) is formulated as DAE index 3, and stabilised via underrelaxation. Navier-Stokes model of viscous incompressible flow is discretised with basic finite volume method on cell-centered collocated mesh arrangement. Displacement of finite volume mesh is modeled via solving elastostatic boundary value problem. The MBS generalized forces pertinent to the aerodynamic loads, after being calculated at the current deformed configuration of the aeroelastic interface, are reduced to mass center of the corresponding rigid body. The A-stable backward differencing formula is used to integrate both the fluid and MBS equations in time. In this paper, we focus ourselves on the spatial coupling, meaning that principle of virtual work (i.e. for small time steps) is adopted in the analysis. A spatial coupling algorithm applied on the aeroelastic interface is formulated as a combination of the rigid and deformable regions. Rigid regions spread on majority of each body in MBS, while deformable part of the aeroelastic interface is used to connect rigid bodies. The problem is observed in 2D, using a model of a wing with control surface in fluid flow, but the formulation is general so it is extendable to 3D.

1 Introduction

In the linear theory of aeroelasticity, the aeroelastic system is modeled as a coupled mathematical system where the structural and aerodynamic part co-exist within the same mathematical model. This approach has been successfully applied within the framework of the classic flutter analysis [3, 14], where the criterion for flutter prediction is established in the frequency domain.

In the time domain, two distinct approaches for numerical treatment of the aeroelastic problems can be identified. Within the *monolithic* approach, the coupled equations that govern fluid–structure interaction (FSI) are discretized and solved within the same solver, so the monolithic approach leads to the fully coupled numerical solution. Drawback is that partitions posses different dynamic characteristics and generally requires different numerical technique.

Different way of modeling leads to the *partitioned* approach, where the flow and structure domains are treated separately within the integration process. These techniques permit independent use of the suitable discretization methods for the different partitions. In partitioned approach we distinguish weak and strong coupled ones. Strong coupling is achieved by solving fixed-point problem either with Picard iterations usually just underrelaxed or via Aitken-type acceleration technique [19], or with Newton-like method with approximate or exact Jaco-

bian [12, 18, 13, 11, 25]. In weak coupling only one solution for both fluid and structural partition is sought in each time step. Generally, overall conservation of forces and transferred energy in partitioned algorithm depend both on the time and the spatial coupling used, and it cannot be investigated separately.

The focus of this paper is on the spatial coupling. This approach is based on conservation of loads and virtual work over the interface. In context of MBS, conservation is considered at global (MBS as a whole), as well as on local level, for (every body in MBS).

For completeness, other components of partitioned FSI formulation are briefly overviewed. Since the fluid domain boundaries undergo a considerable motion, the fluid dynamics equations are to be solved on the dynamic mesh. For this purpose, the Navier–Stokes equations are written in the Arbitrary Lagrangian–Eulerian (ALE) form, which is used for the formulation of the governing equations of FSI as a three–field problem [8].

In three–field formulation, beside the flow field and the deforming mesh, structure partition is often represented by elastic body. For an elastic body on the structural side, the positivity of the deformation gradient tensor determinant is ensuring that structural field has no topological discontinuities. When MBS is on the structural side, parts of the boundary, that is in vicinity of body joints, need special attention since MBS may pose surface topological discontinuity (if we are not interested on discretising finest gaps in structural system). In this paper, radial basis function interpolation is used to represent elastic pseudo-structure surrounding the joints, in order to cope with surface topological discontinuities that MBS can generate (on the flow scales of interest) during the motion.

The paper is organized as follows. In next section FSI algorithm is overviewed, with exception of spatial coupling. Spatial aeroelastic coupling is considered in third section. Finally, the paper ends with an example and conclusion.

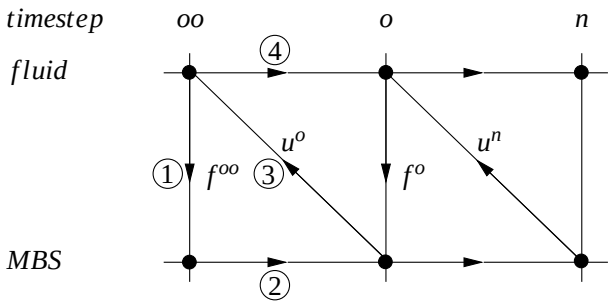

Figure 1: Conventional Serial Staggering (CSS).

2 Fluid–structure interaction

A weakly coupled partitioned algorithm is depicted schematically in 1. Used CSS method renders simulation first order consistent in time, and spatial interface is considered in virtual displacement terms. Loads and displacements are explicitly exchanged at every time step.

2.1 Index 3 formulation of nonlinear multibody dynamical systems

By putting together Lagrangian equations of the first type:

$$\begin{gathered} \mathbf{M}(\mathbf{x})\ddot{\mathbf{x}} + \mathbf{\Phi}_{\mathbf{x}}^{*T}(\mathbf{x},t)\,\boldsymbol{\lambda} = \mathbf{Q}(\dot{\mathbf{x}},\mathbf{x},t) \\ \mathbf{x} \in \mathbb{R}^n\,, \quad \mathbf{\Phi}_{\mathbf{x}}^{*} \in \mathbb{R}^{r\times n}\,, \quad \operatorname{rank}[\mathbf{\Phi}_{\mathbf{x}}^{*}] = r\,, \end{gathered} \tag{1}$$

and the kinematical constraint equations at the position level:

$$\mathbf{\Phi}(\mathbf{x},t) = \mathbf{0}\,, \quad \mathbf{\Phi}(\mathbf{x},t) : \mathbb{R}^n \times \mathbb{R} \to \mathbb{R}^r\,, \tag{2}$$

mathematical model of non-linear constrained multibody dynamical system (MBS) can be established as differential-algebraic system (DAE) of index 3 in the general form (see i.e. [23]):

$$\begin{gathered} \mathbf{M}(\mathbf{x})\ddot{\mathbf{x}} + \mathbf{\Phi}_{\mathbf{x}}^{*T}(\mathbf{x},t)\,\boldsymbol{\lambda} = \mathbf{Q}(\dot{\mathbf{x}},\mathbf{x},t) \\ \mathbf{\Phi}(\mathbf{x},t) = \mathbf{0}\,. \end{gathered} \tag{3}$$

System configuration space is restricted by imposing holonomic constraints (2) at the position level.

Finding the numerical solution of (3), with given initial conditions, that have to satisfy (2),

is not a trivial task. It is well known that some widely used second order accurate numerical schemes, which are unconditionally stable in a linear problems, lead to the numerical instability when applied to DAE index 3 problem, equation (3). The algebraic constraints contained in (3) can be "trigger" for this instability that manifest itself via increasing oscillations in the acceleration response. Actually, index 3 DAE system of the equations (3) can be understood as an ultimate case of the numerically stiff systems with some frequencies taking an infinite value. For this class of the systems, different energy preserving and decaying schemes that exhibit different kinds of the robust time–stepping characteristics for the stiff equations in nonlinear structural dynamics and multibody dynamics are reported in the literature [4]. In this paper DAE system of index 3, equations (3), is integrated in time by means of A-stable backward differencing formula and solution process is stabilised by underrelaxation of both accelerations and velocities.

It is here to be noted that choice of MBS formulation is not essential for whole aeroelastic formulation used in this work, so the aeroelastic interface described in section 3 can be used in a straightforward way also if MBS is formulated in e.g. DAE index 1 mathematical form.

2.2 Discretisation of a flow field

Incompressible isothermal homogeneous flow of Newtonian fluid is described by the Navier–Stokes equations, which are in ALE integral form written as:

$$\begin{aligned} \oint_{\partial V} \boldsymbol{v}\cdot\boldsymbol{n}\,\mathrm{d}S &= 0,\\ \frac{\mathrm{d}}{\mathrm{d}t}\int_V \boldsymbol{v}\,\mathrm{d}V + \oint_{\partial V}\boldsymbol{v}(\boldsymbol{v}-\boldsymbol{v}_s)\cdot\boldsymbol{n}\,\mathrm{d}S &= \oint_{\partial V}\nu(\nabla\boldsymbol{v})\cdot\boldsymbol{n}\,\mathrm{d}S \\ &\quad - \int_V \nabla p\,\mathrm{d}V. \end{aligned} \tag{4}$$

The variable $\boldsymbol{v}_s$ denotes boundary surface velocity, $\boldsymbol{v}$ the fluid velocity, $\boldsymbol{n}$ a unit normal of the boundary surface, ν is the kinematic viscosity and $p := \frac{p}{\rho}$ is "kinematic" pressure .

The geometrical conservation law [8] (also called space conservation law [7]):

$$\frac{\mathrm{d}}{\mathrm{d}t}\int_V \mathrm{d}V = \oint_{\partial V}\boldsymbol{v}_s\cdot\boldsymbol{n}\,\mathrm{d}S, \tag{5}$$

must be satisfied in order to avoid spurious oscillations [8, 9], and is solved together with the Navier–Stokes equations (4). Formally, system of equations (4) and (5) can be written as:

$$\begin{aligned} \frac{\mathrm{d}}{\mathrm{d}t}\int_V \mathrm{d}V + \oint_{\partial V}(\boldsymbol{v}-\boldsymbol{v}_s)\cdot\boldsymbol{n}\,\mathrm{d}S &= 0,\\ \frac{\mathrm{d}}{\mathrm{d}t}\int_V \boldsymbol{v}\,\mathrm{d}V + \oint_{\partial V}\boldsymbol{v}(\boldsymbol{v}-\boldsymbol{v}_s)\cdot\boldsymbol{n}\,\mathrm{d}S &= \oint_{\partial V}\nu(\nabla\boldsymbol{v})\cdot\boldsymbol{n}\,\mathrm{d}S \\ &\quad - \int_V \nabla p\,\mathrm{d}V. \end{aligned}$$

Obtained mathematical model is discretised by basic finite volume (FV) method on the cell–centered co–located grid arrangement.

The coupling of velocity and pressure field on collocated grid arrangement is accomplished by an approximate projection method in spirit of Rhie-Chow [20] (see e.g. [26]).

2.3 Mesh deformation

In this paper cell–centered basic finite volume method is used also for the mesh deformation calculation. In order to represent aeroelastic boundary, the mesh displacement is prescribed at the vertices and then naturally interpolated to the boundary cell faces. In the rest of the fluid domain the mesh displacement is solved for and interpolated from cell centers to vertices.

In order to determine FV mesh deformation during the coupled aeroelastic simulation, the Lamé–Navier boundary value problem for the elastostatic body is solved in every time step for the given boundary displacement.

In the case of isotropic and homogeneous linear elastic body in the absence of body forces, the static equilibrium equation is given by:

$$\int_V \nabla \cdot \boldsymbol{\sigma}_M \, \mathrm{d}V = 0, \tag{6}$$

where $\boldsymbol{\sigma}_M = 2\mu\boldsymbol{\epsilon} + \lambda \operatorname{tr}(\boldsymbol{\epsilon})\boldsymbol{I}$ is Caushy stress tensor. The Lamé coefficients represent characteristics of the material, and must satisfy conditions $\mu > 0$ and $3\lambda + 2\mu > 0$, and the infinitesimal deformation tensor is $\boldsymbol{\epsilon} = \frac{1}{2}\left(\nabla\boldsymbol{u} + (\nabla\boldsymbol{u})^T\right)$. Now we can obtain Lamé–Navier equation, an elastostatic equation (6) in terms of displacement field $\boldsymbol{u}$, which is used for the mesh deformation calculation:

$$\int_V \nabla \cdot \left[\mu\nabla\boldsymbol{u} + \mu(\nabla\boldsymbol{u})^T + \lambda\,(\nabla\cdot\boldsymbol{u})\boldsymbol{I}\right] \, \mathrm{d}V = 0. \tag{7}$$

Each component of the displacement is solved separately, and inter-component coupling terms are treated explicitly in the dimensional splitting procedure. Consequently it is necessary to iterate over the inter–component coupling, however the convergence is speed up [15] by use of decomposition of deformation gradient tensor on its symmetric and skew-symmetric part:

$$\begin{aligned} &\oint_{\partial V} 2\mu\nabla\boldsymbol{u}\cdot\boldsymbol{n}\,\mathrm{d}S = \\ &\oint_{\partial V} \left[\mu\left(\nabla\boldsymbol{u} - (\nabla\boldsymbol{u})^T\right) - \lambda\,(\nabla\cdot\boldsymbol{u})\boldsymbol{I}\right]\cdot\boldsymbol{n}\,\mathrm{d}S, \end{aligned} \tag{8}$$

where $\nabla\cdot\boldsymbol{u}$ is calculated as $\operatorname{tr}(\nabla\boldsymbol{u})$ since interpolation of $\nabla\boldsymbol{u}$ in FV faces is used to calculate other terms, and is already in memory of a computer in that stage. In the equation (8) the left side is treated implicitly, while the source on the right hand side calculated explicitly.

On the stationary parts of a mesh boundary, either fixed or slip boundary condition are prescribed. In Lamé–Navier boundary value problem mesh is fixed on boundary with Dirichlet boundary condition:

$$\boldsymbol{u} = \boldsymbol{0} \quad \text{on } \Gamma_{fixed}.$$

The slip boundary condition is obtained by prescribing Neumann boundary condition for the tangential component of the displacement:

$$\left(\nabla\left[(\boldsymbol{I} - \boldsymbol{n}\boldsymbol{n})\cdot\boldsymbol{u}\right]\right)\cdot\boldsymbol{n} = \boldsymbol{0} \quad \text{on } \Gamma_{slip},$$

while for the normal component of the displacement Dirichlet boundary condition is used:

$$\boldsymbol{u}\cdot\boldsymbol{n} = 0 \quad \text{on } \Gamma_{slip}.$$

The slip boundary condition is preferable because it allows mesh to rotate more freely with the structural system, so less deformed mesh is produced during simulation. By allowing mesh to slip on the upper and lower boundary while fixing it at the inlet and outlet, a robust procedure is obtained.

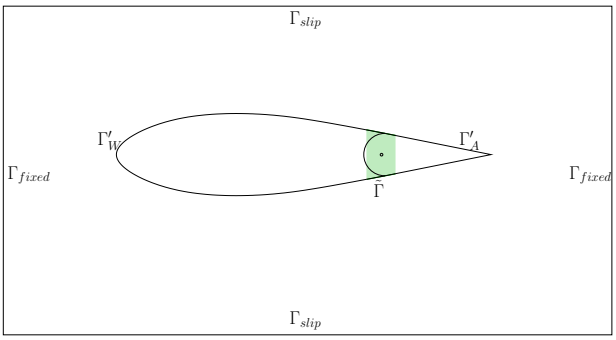

Figure 2: $\Gamma = \Gamma'_W \cup \tilde{\Gamma} \cup \Gamma'_A$, and $\tilde{\Gamma} = \tilde{\Gamma}_W \cup \tilde{\Gamma}_A$. Green dashed region is elastic part of MBS "field".

Now focus can be turned to description of the spatial aeroelastic interface.

3 Spatial aeroelastic coupling

During the motion, a surface of the structural system may experience topological changes. For example, point at the aileron in the neighborhood of the wing might be exposed to the fluid flow in one moment and then sunk into the gap (behind the wing) in the next one. So, in order to move fluid mesh on the FSI interface, a method is needed that can robustly cope with

the moderate changes of the interface topology. For this purpose, due to flexibility with respect of problem dimensionality and data centers distribution, Radial Basis Function (RBF) interpolation of Lagrangian data is used in the framework of this analysis.

In contrast to the work done in [22], where all MBS was represented with RBF interpolation (RBFI) as one deformable pseudo-body, here the surface is mapped rigidly on majority of aeroelastic interface. In this paper a RBFI is used to patch between the rigid bodies of MBS only near the hinge that connects airfoil and control surface (see fig 2). That zone, which spreads on both bodies, absorbs topological discontinuities that occur in vicinity of the control surface joint. By following this route, elastic deformation is localized to a minor part of FSI interface.

RBFI is defined at any point occupied by MBS. Since discontinuities are absorbed with in RBFI as continuous deformations, also when dealing with RBFI as representation of MBS it make sense to speak about three–field aeroelastic formulation. Here points that represent MBS can be taken e.g. coarsened from FSI fluid mesh boundary. As major parts of FSI interface are mapped rigidly, one has to "zip up" rigid-to-deformable transition regions of the interface with data centers that coincide with FV mesh vertices. RBFI patches, between any two connected rigid parts, are best chosen as small as possible, but large enough to cope with topology changes that MBS boundary will encounter during simulation of flow field scales of interest. In this paper MBS is represented in a three–field formulation, as simply connected region in fluid mesh.

Unlike some other methods used to define the aeroelastic interface, such as the nearest neighbor method [24] or the weighted residual method [16, 17, 5], when using a RBFI no orthogonal projection is needed to create the aeroelastic interface.

3.1 Consistent and conservative aeroelastic interface

Firstly, let us adopt terminology conveniently used in [6] for spatial coupling of aeroelastic problems. As defined in [6], a consistent interface is one that trensfers loads from constant pressure exactly, but is not necessary conservative in sense introduced in [10]. On the other hand, conservative aeroelastic interface is one that conserves the virtual work globally. As shown in [10], global virtual conservativeness is achieved by using $\mathbf{H}^T$ transfer matrix for loads, if transfer matrix $\mathbf{H}$ is used for displacement. However, by using RBFI in that approach, an effect of unphysical oscillations in the transfered load field might arise [2, 6]. When dealing with elastic bodies that effect pose a problem. It also pose the problem when dealing with MBS on structural side, and RBFI part is shared between bodies, since there are no means to guarantee that forces (and moments in MBS problem) are the same on both side of the RBFI aeroelastic interface for each body in MBS. Loads can be enforced the same on both sides of the aeroelastic interface only globally, on MBS as a whole.

It is usually more important to have equal forces and moments on each body in MBS than to conserve virtual work, since wrong forces or moments would affect dynamics of MBS. Furthermore, non-conservativeness of aeroelastic interface does not necessary affect the stability and accuracy of the computation [6]. When spatial and temporal discretization of partitions are dissipative enough, the coupling error introduced by information transfer is smaller then the spatial and temporal discretization error. However, when the stability becomes an issue, the difference of energy caused by non matching interface should be such that MBS receives less energy than is taken from a fluid.

In this paper consistent approach of constructing FSI interface will be used, with consideration to the rigid bodies MBS particularities. So, to obtain the consistent interface, a constant pressure should be exactly transfered over the inter-

face in terms of resulting force and moment.

3.2 Rigid aeroelastic interface

On a body with boundary Γ, surface force and moment around point O are:

$$\begin{aligned} \boldsymbol{R}_F &= \oint_\Gamma \boldsymbol{\sigma}\cdot\boldsymbol{n}\,\mathrm{d}S, \\ \boldsymbol{R}_M &= \oint_\Gamma \tilde{\boldsymbol{r}}\times(\boldsymbol{\sigma}\cdot\boldsymbol{n})\,\mathrm{d}S, \end{aligned} \tag{9}$$

where $\tilde{\boldsymbol{r}} = \boldsymbol{r} - O$, and $\boldsymbol{\sigma} = -p\boldsymbol{I} + \mu\left[\nabla\boldsymbol{v} + (\nabla\boldsymbol{v})^T\right]$. If we discretise (9) consistently with FVM, in sense [6] ($\boldsymbol{\sigma}(\boldsymbol{x}) = -p = \text{const}$) we obtain:

$$\begin{aligned} \boldsymbol{R}_F &= -p\sum_{i\in\Gamma_F}\boldsymbol{n}_i A_i, \\ \boldsymbol{R}_M &= -p\sum_{i\in\Gamma_F}\tilde{\boldsymbol{r}}_i\times\boldsymbol{n}_i A_i. \end{aligned} \tag{10}$$

More generally, FVM consistent discretization is [1]:

$$\begin{aligned} \boldsymbol{R}_F &= \sum_{i\in\Gamma_F}\mathfrak{F}_i A_i = \sum_{i\in\Gamma_F}\boldsymbol{f}_i, \\ \boldsymbol{R}_M &= \sum_{i\in\Gamma_F}\tilde{\boldsymbol{r}}_i\times\mathfrak{F}_i A_i = \sum_{i\in\Gamma_F}\tilde{\boldsymbol{r}}_i\times\boldsymbol{f}_i, \end{aligned} \tag{11}$$

where $\tilde{\boldsymbol{r}}_i$ is a point on boundary face i of fluid side of discrete aeroelastic interface Γ_F, and $\mathfrak{F}_i = \boldsymbol{\sigma}_i\cdot\boldsymbol{n}_i$. In this paper $\tilde{\boldsymbol{r}}_i$ is centroid of the boundary face i.

Next, we will show that consistent approach on a rigid interface is conservative. The motion of any point $\boldsymbol{r}'$ fixed on a rigid body can be written as [1] $\boldsymbol{r}(t) = \boldsymbol{r}_O(t) + \boldsymbol{Q}(t)\boldsymbol{r}'$. Now, at any time t, for point $\boldsymbol{r}'$ on a rigid body, infinitesimal rigid displacement is of a form:

$$\delta\boldsymbol{u} = \delta\boldsymbol{u}_O + (\boldsymbol{Q}(\boldsymbol{\delta}) - \boldsymbol{I})\boldsymbol{Q}(t)\boldsymbol{r}', \tag{12}$$

where $\boldsymbol{Q}(\boldsymbol{\delta})$ is orthogonal tensor of infinitesimal rotation $\boldsymbol{\delta}$.

[1] Order of consistency is not in focus of this paper.

Since infinitesimal rotations can be written in the form $\boldsymbol{Q} = \boldsymbol{I} + \boldsymbol{A}$, where $\boldsymbol{A}\in Skew$, a virtual rigid displacement can be rewritten as:

$$\delta\boldsymbol{u} = \delta\boldsymbol{u}_O + \boldsymbol{A}(\boldsymbol{\delta})\,\tilde{\boldsymbol{r}}(t), \tag{13}$$

where $\tilde{\boldsymbol{r}}(t) = \boldsymbol{Q}(t)\boldsymbol{r}'$, and $\boldsymbol{\delta}$ is axial vector of the operator $\boldsymbol{A}(\boldsymbol{\delta})$. Now, for any point $\boldsymbol{r}'_i$ on the rigid body, a virtual displacement is $\delta\boldsymbol{u}_i = \delta\boldsymbol{u}_O + \boldsymbol{A}(\boldsymbol{\delta})\,\tilde{\boldsymbol{r}}_i(t)$.

For the rigid interface to be conservative for a virtual work on discrete level, it is enough to show that:

$$\begin{bmatrix}\delta\boldsymbol{u}_1 & \delta\boldsymbol{u}_2 & \dots & \delta\boldsymbol{u}_n\end{bmatrix}\cdot\begin{bmatrix}\boldsymbol{f}_1\\ \boldsymbol{f}_2\\ \vdots\\ \boldsymbol{f}_n\end{bmatrix} = \begin{bmatrix}\delta\boldsymbol{u}_O & \boldsymbol{\delta}\end{bmatrix}\cdot\begin{bmatrix}\boldsymbol{R}_F\\ \boldsymbol{R}_M\end{bmatrix}. \tag{14}$$

The conservativeness is easily proven by a simple calculation. By use of equation (13), we can write left hand side of (14) as:

$$\begin{aligned} \sum_{i\in\Gamma_F}\delta\boldsymbol{u}_i\cdot\boldsymbol{f}_i &= \sum_{i\in\Gamma_F}(\delta\boldsymbol{u}_O + \boldsymbol{A}(\boldsymbol{\delta})\,\tilde{\boldsymbol{r}}_i)\cdot\boldsymbol{f}_i \\ &= \sum_{i\in\Gamma_F}\delta\boldsymbol{u}_O\cdot\boldsymbol{f}_i + \sum_{i\in\Gamma_F}(\boldsymbol{A}(\boldsymbol{\delta})\,\tilde{\boldsymbol{r}}_i)\cdot\boldsymbol{f}_i \\ &= \delta\boldsymbol{u}_O\cdot\sum_{i\in\Gamma_F}\boldsymbol{f}_i + \boldsymbol{\delta}\cdot\sum_{i\in\Gamma_F}\boldsymbol{A}(\tilde{\boldsymbol{r}}_i)\boldsymbol{f}_i \\ &= \delta\boldsymbol{u}_O\cdot\boldsymbol{R}_F + \boldsymbol{\delta}\cdot\boldsymbol{R}_M. \quad Q.E.D. \end{aligned} \tag{15}$$

In (15), next to last equality follows from properties of triple (mixed scalar-vector) product, and last from equations (11).

If we write equation (13) for every point in matrix form, with use of the identity $\boldsymbol{A}(\boldsymbol{\delta})\tilde{\boldsymbol{r}}_i = -\boldsymbol{A}(\tilde{\boldsymbol{r}}_i)\boldsymbol{\delta}$, we obtain displacement transfer matrix $\mathbf{H}$:

$$\begin{bmatrix}\delta\boldsymbol{u}_1\\ \delta\boldsymbol{u}_2\\ \vdots\\ \delta\boldsymbol{u}_n\end{bmatrix} = \begin{bmatrix}\boldsymbol{I} & -\boldsymbol{A}(\tilde{\boldsymbol{r}}_1)\\ \boldsymbol{I} & -\boldsymbol{A}(\tilde{\boldsymbol{r}}_2)\\ \vdots & \vdots\\ \boldsymbol{I} & -\boldsymbol{A}(\tilde{\boldsymbol{r}}_n)\end{bmatrix}\begin{bmatrix}\delta\boldsymbol{u}_O\\ \boldsymbol{\delta}\end{bmatrix} = \mathbf{H}\begin{bmatrix}\delta\boldsymbol{u}_O\\ \boldsymbol{\delta}\end{bmatrix}. \tag{16}$$

Now it is easy to see that loads are transfered from a rigid body with $\mathbf{H}^T$:

$$\begin{bmatrix} \boldsymbol{I} & \boldsymbol{I} & \dots & \boldsymbol{I} \\ \boldsymbol{A}(\tilde{\boldsymbol{r}}_1) & \boldsymbol{A}(\tilde{\boldsymbol{r}}_2) & \dots & \boldsymbol{A}(\tilde{\boldsymbol{r}}_n) \end{bmatrix} \begin{bmatrix} \boldsymbol{f}_1 \\ \boldsymbol{f}_2 \\ \vdots \\ \boldsymbol{f}_n \end{bmatrix} = \begin{bmatrix} \sum_i \boldsymbol{f}_i \\ \sum_i \boldsymbol{A}(\tilde{\boldsymbol{r}}_i)\boldsymbol{f}_i \end{bmatrix} = \begin{bmatrix} \boldsymbol{R}_F \\ \boldsymbol{R}_M \end{bmatrix}. \quad (17)$$

Mesh displacement is being prescribed at mesh vertices, and generally is mollified when calculated in FV polygonal face center. As a consequence, when using conservative approach with e.g. cell–centered collocated FVM, as load is calculated at FV face centers, and displacement is prescribed at the vertices of the FV mesh, so generally only approximative conservation is archived. It is trivial to show that, when interface is rigid it is not important that points for load calculation and mesh displacement prescription do not coincide since whole interface is moving rigidly. It is so even if boundary points for pressure (spherical part), and boundary points at which deviatoric part of stress tensor is calculated do not coincide, as long as all boundary points move on the rigidly with the interface.

3.3 Radial basis function interpolation aeroelastic interface

For parts of interface that undergoes topological changes, RBFI is used to interpolate displacement, so RBFI interface is used to "patch" zones between rigid parts of the interface.

Firstly we will define two sets of points, $Y = \{\boldsymbol{y}_1, \boldsymbol{y}_2, ..., \boldsymbol{y}_{|Y|}\}$ and $X = \{\boldsymbol{x}_1, \boldsymbol{x}_2, ..., \boldsymbol{x}_{|X|}\}$ are structural and fluid mesh points respectively, that represent RBF part of FSI boundary, where number of the structural and fluid mesh points is denoted with $|Y|$ and $|X|$ respectively. Without arising ambiguity, set of indexes of those point sets will be denoted with same letters, X and Y.

In those two sets of points discrete displacement is defined as $\mathbf{U} = \boldsymbol{u}|_X$ and $\mathbf{u} = \boldsymbol{u}|_Y$.

Now, for any direction d of $|\mathcal{D}|$ dimensional space [2], the radial basis function interpolation of displacement, if done by using Lagrangian data, can be written of the form [27]:

$$s(\boldsymbol{x}) = \sum_{j \in Y} \alpha_j \varphi(|\boldsymbol{x} - \boldsymbol{y}_j|_2) + \sum_{j \in \Pi} \beta_j \pi_j(\boldsymbol{x}), \quad (18)$$

where $\varphi : \mathbb{R}^{|\mathcal{D}|} \to \mathbb{R}$ is (conditionally) positive definite function of order m and $\pi \in \Pi_{m-1}(\mathbb{R}^{|\mathcal{D}|})$ is $|\mathcal{D}|$-variate polynomial of degree at most $m-1$.

The coefficients α_j and β_j will be determined from the interpolation condition for any of the $d \in \mathcal{D}$:

$$s(\boldsymbol{y}_j) = u_j, \quad j \in Y. \quad (19)$$

After imposing orthogonality condition:

$$\sum_{j \in Y} \alpha_j q(\boldsymbol{y}_j) = 0, \quad \forall q \in \Pi_{m-1}(\mathbb{R}^{|\mathcal{D}|}),$$

the interpolation is unique if the structural points $\boldsymbol{y}_j$ form an uni-solvent system for the polynomials. Consequence of that orthogonality in the RBFI interface is that for constant polynomial translations are recovered exactly. By using the linear polynomial, infinitesimal rotations are recovered exactly also. For load, as conjugated aeroelastic variable, forces and moments are the same on both sides of the conservative interface when constant and linear polynomials are used respectively.

Now, interpolation problem, equations (18) and (19), can be written in the form:

$$\begin{bmatrix} \mathbf{A}_{YY} & \mathbf{P}_Y \\ \mathbf{P}_Y^T & \mathbf{0} \end{bmatrix} \begin{bmatrix} \boldsymbol{\alpha} \\ \boldsymbol{\beta} \end{bmatrix} = \begin{bmatrix} \mathbf{u} \\ \mathbf{0} \end{bmatrix}, \quad (20)$$

where $\mathbf{u}$ is discrete value of interface displacement $\boldsymbol{u}(\boldsymbol{x})$ and is imposed on the structural side of aeroelastic interface, and $\mathbf{A}_{YY} = \varphi(|\boldsymbol{y}_i - \boldsymbol{y}_j|_2) \in \mathbb{R}^{|Y| \times |Y|}$ and $\mathbf{P}_Y = \pi_k(\boldsymbol{y}_i) \in \mathbb{R}^{|Y| \times Q}$. Now the discrete values of displacement interpolant (18) are calculated at evaluation points

[2] Set of indexes that correspond to unit base vectors will be denoted with $\mathcal{D}$, and its cardinal number $|\mathcal{D}|$ is dimensionality of used Euclidean space.

X via coefficients given in (20):

$$\begin{aligned} \boldsymbol{s}|_X &= \begin{bmatrix} \mathbf{A}_{XY} & \mathbf{P}_X \end{bmatrix} \begin{bmatrix} \mathbf{A}_{YY} & \mathbf{P}_Y \\ \mathbf{P}_Y^T & \mathbf{0} \end{bmatrix}^{-1} \begin{bmatrix} \mathbf{u} \\ \mathbf{0} \end{bmatrix} \\ &= \begin{bmatrix} \mathbf{H} & \tilde{\mathbf{H}} \end{bmatrix} \begin{bmatrix} \mathbf{u} \\ \mathbf{0} \end{bmatrix}. \end{aligned} \tag{21}$$

In the equation (21), $\mathbf{A}_{XY} = \varphi(|\boldsymbol{x}_i - \boldsymbol{y}_j|_2) \in \mathbb{R}^{|X|\times|Y|}$, $\boldsymbol{P}_X = \pi_j(\boldsymbol{y}_i) \in \mathbb{R}^{|X|\times Q}$, and $\mathbf{H} \in \mathbb{R}^{|X|\times|Y|}$ is the displacement transfer matrix. Now, the displacement of the fluid mesh points can be obtained from:

$$\mathbf{U}_d = \mathbf{H}\mathbf{u}_d, \quad d \in \mathcal{D}, \tag{22}$$

The Wendland's C^2 class function with the compact support is chosen for φ. For 2D and 3D problems it is defined as $\varphi(r) = (1-r)_+^4(1+4r)$, where $r = \frac{|\boldsymbol{x}-\boldsymbol{y}_j|_2}{\delta}$ is normalized Euclidean distance, and δ is support radius.

3.3.1 Consistent RBFI interface

The method will be illustrated by example shown in the Figure 3. Let MBS be consisted of the two bodies (wing and aileron) and let data centers and the evaluation points are separated accordingly: $Y = \{w, a\}$ and $X = \{W, A\}$. Then the coefficients $\boldsymbol{\alpha}$ and $\boldsymbol{\beta}$ given in (20) can be calculated by the expression:

$$\begin{bmatrix} \boldsymbol{\alpha}_w \\ \boldsymbol{\alpha}_a \\ \boldsymbol{\beta} \end{bmatrix} = \begin{bmatrix} \mathbf{A}_{ww} & \mathbf{A}_{aw} & \mathbf{P}_w \\ \mathbf{A}_{aw}^T & \mathbf{A}_{aa} & \mathbf{P}_a \\ \mathbf{P}_w^T & \mathbf{P}_a^T & \mathbf{0} \end{bmatrix}^{-1} \begin{bmatrix} \mathbf{u}_w \\ \mathbf{u}_a \\ \mathbf{0} \end{bmatrix},$$

or the displacement transfer matrix is used to interpolate fluid mesh boundary displacement (see equation (21)):

$$\begin{aligned} &\begin{bmatrix} \mathbf{U}_W \\ \mathbf{U}_A \end{bmatrix} \\ &= \begin{bmatrix} \mathbf{A}_{Ww} & \mathbf{A}_{Wa} & \mathbf{P}_W \\ \mathbf{A}_{Aw} & \mathbf{A}_{Aa} & \mathbf{P}_A \end{bmatrix} \begin{bmatrix} \mathbf{A}_{ww} & \mathbf{A}_{aw} & \mathbf{P}_w \\ \mathbf{A}_{aw}^T & \mathbf{A}_{aa} & \mathbf{P}_a \\ \mathbf{P}_w^T & \mathbf{P}_a^T & \mathbf{0} \end{bmatrix}^{-1} \begin{bmatrix} \mathbf{u}_w \\ \mathbf{u}_a \\ \mathbf{0} \end{bmatrix} \cdot \begin{bmatrix} \mathbf{f}_w \\ \mathbf{f}_a \\ \mathbf{0} \end{bmatrix} \end{aligned} \tag{23}$$

In the consistent approach the aerodynamic loads are then transfered by means of equations (11).

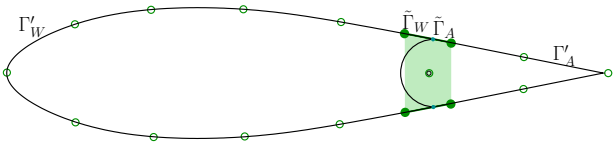

Figure 3: Blue dots indicate regions which are topological singularities during aileron deflection. Green circles represent Lagrangian data centers, and green dots represent data centers which coincide with finite volume mesh vertices. Green dashed region represents the elastic part of the MBS field.

3.3.2 Conservative radial basis function interpolation interface

The general opinion is that virtual work should be conserved over the interface. This is accomplished by using transposed displacement transfer matrix for load transfer matrix:

$$\mathbf{f}_d = \mathbf{H}^T\mathbf{F}_d, \quad d \in \mathcal{D}, \tag{24}$$

where $\mathbf{F}_d$ and $\mathbf{f}_d$ are loads on fluid and structural side respectively.

In FSI problem with MBS, the loads could be transfered conservatively such that they are first transfered by means of equation (24) to the points used for mesh deformation (green circles on fig 3), and then reduced from this points to mass center of every body in MBS that corresponds to given part of the interface defined at some reference configuration. Then one could rewrite equation (24), by the use of (23), to obtain load transfer matrix for the example used in this paper:

$$\begin{aligned} &= \begin{bmatrix} \mathbf{A}_{ww} & \mathbf{A}_{aw} & \mathbf{P}_w \\ \mathbf{A}_{aw}^T & \mathbf{A}_{aa} & \mathbf{P}_a \\ \mathbf{P}_w^T & \mathbf{P}_a^T & \mathbf{0} \end{bmatrix}^{-1} \begin{bmatrix} \mathbf{A}_{Ww}^T & \mathbf{A}_{Aw}^T \\ \mathbf{A}_{Wa}^T & \mathbf{A}_{Aa}^T \\ \mathbf{P}_W^T & \mathbf{P}_A^T \end{bmatrix} \begin{bmatrix} \mathbf{F}_W \\ \mathbf{F}_A \end{bmatrix}, \end{aligned}$$

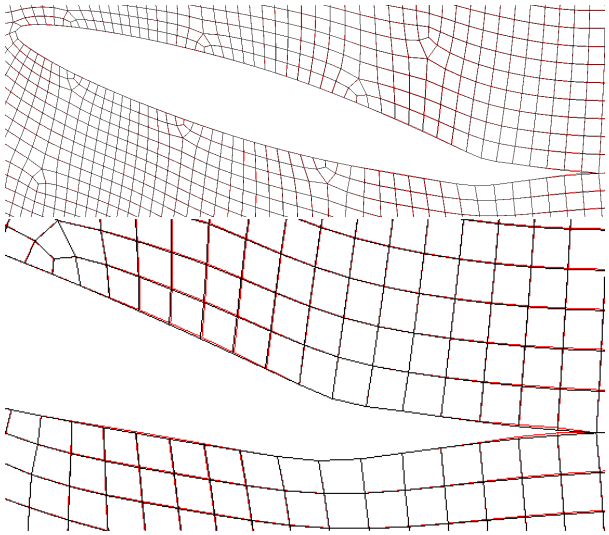

Figure 4: Comparison of methods from [22, 21] where whole aeroelastic interface was deformed via RBFI (red lines), and formulation used in this paper (black lines). For visualization reason highly coarse mesh is used. It can be seen that meshes coincide on RBFI part of the interface, while differing on parts of boundary that is mapped rigidly in this method (with exception of displacement in data centers). Second image is the detail of an aft part of the configuration displayed in the first image.

from which it follows:

$$\begin{bmatrix} \mathbf{A}_{ww} & \mathbf{A}_{aw} & \mathbf{P}_w \\ \mathbf{A}_{aw}^T & \mathbf{A}_{aa} & \mathbf{P}_a \\ \mathbf{P}_w^T & \mathbf{P}_a^T & \mathbf{0} \end{bmatrix} \begin{bmatrix} \mathbf{f}_w \\ \mathbf{f}_a \\ \mathbf{0} \end{bmatrix} = \begin{bmatrix} \mathbf{A}_{wW} & \mathbf{A}_{wA} \\ \mathbf{A}_{aW} & \mathbf{A}_{aA} \\ \mathbf{P}_W^T & \mathbf{P}_A^T \end{bmatrix} \begin{bmatrix} \mathbf{F}_W \\ \mathbf{F}_A \end{bmatrix}. \tag{25}$$

From last equation in system (25), we obtain:

$$\mathbf{P}_w^T \mathbf{f}_w + \mathbf{P}_a^T \mathbf{f}_a = \mathbf{P}_W^T \mathbf{F}_W + \mathbf{P}_A^T \mathbf{F}_A.$$

Thus, forces and moments are the same on both sides of the interface globally for all MBS, but there are no means in this framework to also enforce $\mathbf{P}_b^T \mathbf{f}_b = \mathbf{P}_B^T \mathbf{F}_B$ for each body in MBS, and this would produce wrong MBS dynamics.

4 Numerical example: MBS in fluid flow

The described methodology is applied to the flow induced MBS dynamics in the framework of a weakly coupled simulation of the wing-aileron multibody model. The flow around NACA 65-012 airfoil is laminar, at $Re = 1 \cdot 10^5$. The spatial schemes within the flow solver are central differencing scheme for the diffusive term, and stabilised scheme for the convection. For the data centers of the RBFI interface, a set of points on the wing and aileron was chosen to represent the structural system displacement. In used example, distribution of the points that represent structural system is depicted on fig 3.

5 Conclusion

This paper is part of effort to develop the spatial coupling interface that can be successfully applied for MBS on the structural partition side. For that purpose, consistent RBFI aeroelastic interface is constructed on minor parts of the interface. With the conservative rigid parts, by-major-parts conservative weakly coupled FSI solution algorithm is constructed for the simulation of MBS in viscous incompressible fluid flow. For each partition, a A-stable backward differencing formula is used.

In this paper it was shown for rigid bodies that

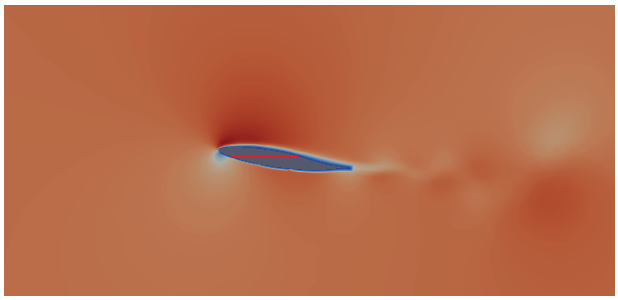

Figure 5: MBS in fluid flow. Red line indicates reference chord position

consistent approach for FSI interface is conservative, in virtual (infinitesimal) terms.

Since well-calculated aerodynamic loads on each body are crucial for the accurate time integration of the MBS, consistent RBFI interface $\tilde{\Gamma} = \tilde{\Gamma}_W \cup \tilde{\Gamma}_A$ is used on minor part of the aeroelastic interface Γ (see fig 2). The generalized forces pertinent to the aerodynamic loads are reduced to center of gravity of the corresponding body, after being calculated at the fluid mesh of an appropriate part of the FSI boundary.

The described methodology is applied for a motion simulation of an airfoil with control surface in incompressible viscous fluid flow. Presented FSI spatial interface can be used both in 2D and 3D, as long as surface topological changes are moderate.

Acknowledgements

Authors acknowledge the support of the Croatian Ministry of Science and Technology through research project "Numerical simulation procedures for elastic airplane landing dynamics, and the Croatian Science Foundation under the contract of the project "Geometric Numerical Integrators on Manifolds for Dynamic Analysis and Simulation of Structural Systems" conducted at Chair of Flight Vehicle Dynamics, Faculty of Mechanical Engineering and Naval Architecture, University of Zagreb.

References

[1] Ibrahim Aganović. *An introduction to analytical mechanics*. PMF, Uni. Zagreb, 1990. Manualia Universitatis studiorum Zagrabiensis, in Croatian.

[2] A. Ahrem, A. Beckert, and H. Wendland. A new multivariate interpolation method for large-scale coupling problems in aeroelasticity for the coupling of non-matching meshes. In *Conference Proceedings IFADS*, Munich, Germany, 2005.

[3] R.L. Bisplinghoff, H. Ashley, and R.L. Halfman. *Aeroelasticity*. Dover Publications, New York, 1955.

[4] C.L. Bottasso and L. Trainelli. An attempt at the classification of energy decaying schemes for structural and multibody dynamics. *Multibody System Dynamics*, 12:173–185, 2004.

[5] J. Cebral and R. Löhner. Conservative load projection and tracking for fluid-structure problems. *AIAA J.*, 35 (4):687–692, 1997.

[6] A. de Boer, A. van Zuijlen, and H. Bijl. Comparison of conservative and consistent approaches for the coupling of non-matching meshes. *Computer Methods in Applied Mechanics and Engineering*, 197:4284–4297, 2008.

[7] I. Demirdžić and M. Perić. Space conservation law in finite volume calculations of fluid flow. *International journal for numerical methods in fluids*, 8:1037–1050, 1988.

[8] C. Farhat, M. Lesoinne, and N. Maman. Mixed explicit/implicit time integration of coupled aeroelastic problems: three-field formulation, geometric conservation and distributed solution. *Int J Numer Meths Fluids*, 21:807–835, 1995.

[9] C. Farhat, M. Lesoinne, and N. Maman. Geometric conservation laws for flow problems with moving boundaries and deformable meshes and their impact on aeroelastic computations. *Comput Meths Appl Mech Engng*, 134:71–90, 1996.

[10] C. Farhat, M. Lesoinne, and P. Tallec. Load and motion transfer algotirhms for fluid-structure interaction problems with non-matching discrite interfaces: Momentum and energy conservation, optimal discretisation and application to aeroelasticity. *Comput. Methods Appl. Mech. Engrg.*, 157:95–114, 1998.

[11] M.A. Fernández and M. Moubachir. A newton method using exact jacobians for solving fuid-structure coupling. *Comput. Struct.*, 83:127–142, 2005.

[12] J.F. Gerbeau and M. Vidrascu. A quasinewton algorithm based on a reduced model for fuid structure problems in blood fow. *Mathematical Modelling and Numerical Analysis*, 37:631–647, 2003.

[13] M. Heil. An eient solver for the fully coupled solution of large displacement fluid-structure interaction problems. *Comput. Methods Appl. Mech. Engrg.*, 193:1–23, 2004.

[14] D.H. Hodges. *Introduction to Structural Dynamics and Aeroelasticity*. Cambridge University Press, 2002.

[15] H. Jasak and H.G. Weller. Application of the finite volume method and unstructured meshes to linear elasticity. *International journal for numerical methods in engineering*, 48:267–287, 2000.

[16] R. Löhner, C. Yang, J. Cebral, J.D. Baum, H. Luo, D. Pelessone, and C. Charman. Fluid-structure interaction using a loose coupling algorithm and adaptive unstructured grids. In M. Hafez and K. Oshima, editors, *Computational Fluid Dynamics Review*. John Wiley, 1995.

[17] N. Maman and C. Farhat. Matching fluid and structure meshes for aeroelastic computations: A parallel approach. *Comput. Struct.*, 54 (4):779–785, 1995.

[18] H.G. Matthies and J. Steindorf. Partitioned strong coupling algorithms for fuid structure interaction. *Comput. Struct.*, 81:805–812, 2003.

[19] D.P. Mok, W.A. Wall, and E. Ramm. Accelerated iterative substructuring schemes for instationary fluid-structure interaction. In K.J. Bathe, editor, *Computational Fluid and Solid Mechanics*, pages 1325–1328. Elsevier, 2001.

[20] C. M. Rhie and W. L. Chow. Numerical study of the turbulent flow past an airfoil with trailing edge separation. *AIAA Journal*, 21(11):1525–1532, 1983.

[21] Z. Terze, D. Matijašević, and M. Vrdoljak. Numerical fluid-structure interaction of multi-body dynamical systems in incompresible flow. In *Conference Proceedings CMND2009*, Split, Croatia, September 2009.

[22] Z. Terze, D. Matijašević, M. Vrdoljak, and V. Koroman. Fluid-structure interaction in the framework of numerical dynamic simulation of multibody systems. In *Conference Proceedings IFASD*, Seattle, USA, June 2009. IFASD-2009-097.

[23] Z. Terze and J. Naudet. Geometric properties of projective constraint violation stabilization method for generally constrained multibody systems on manifold. *Multibody System Dynamics*, 20:85–106, 2008.

[24] P. Thévenza, T. Blu, and M. Unser. Interpolation revisited. *IEEE Med. Trans. Med. Imag.*, 19 (7):739–758, 2000.

[25] J. A. Vierendeels. Strong coupling of partitioned fluid-structure interaction problems with reduced order models. In *ECCOMAS CFD 2006*, pages 5–18, 2006.

[26] Ž. Tuković and H. Jasak. A moving mesh finite volume interface tracking method for surface tension dominated interfacial fluid flow. *Computers and Fluids*, 55:70–84, 2012.

[27] H. Wendland. *Scattered data approximation*. Cambribge University Press, 2010.